Tokyo Climate Center, Japan Meteorological Agency

TCC News

No. 24 Spring 2011

Contents

El Niño Outlook (April – October 2011)

The La Niña conditions that have persisted since last boreal summer are likely to decay by the end of boreal spring, and subsequent neutral conditions are likely to continue in boreal summer.

Pacific Ocean

In March 2011, the SST deviation from a sliding 30-year mean SST averaged over the NINO.3 region was -0.7°C. The five-month running-mean value of NINO.3 SST deviations was -1.2°C for January, and the Southern Oscillation Index for March was +2.0. In March, SST anomalies were remarkably negative in the central equatorial Pacific, and were positive around Indonesia (Figure 1). Subsurface temperature anomalies were positive in the western and central equatorial Pacific (Figure 2), while negative ocean heat content (OHC) anomalies in its eastern part decreased through March. In late March, positive OHC anomalies prevailed over nearly the whole area of the equatorial Pacific (Figure 3). In the lower troposphere, easterly wind anomalies were seen over the western and central equatorial Pacific. These characteristics indicate decaying La Niña conditions.

Further eastward migration of positive subsurface temperature anomalies in the western and central equatorial Pacific are expected to cause weakening of negative SST anomalies in its eastern part.

JMA's El Niño prediction model forecasts that the NINO.3 SST will be near normal during boreal spring and

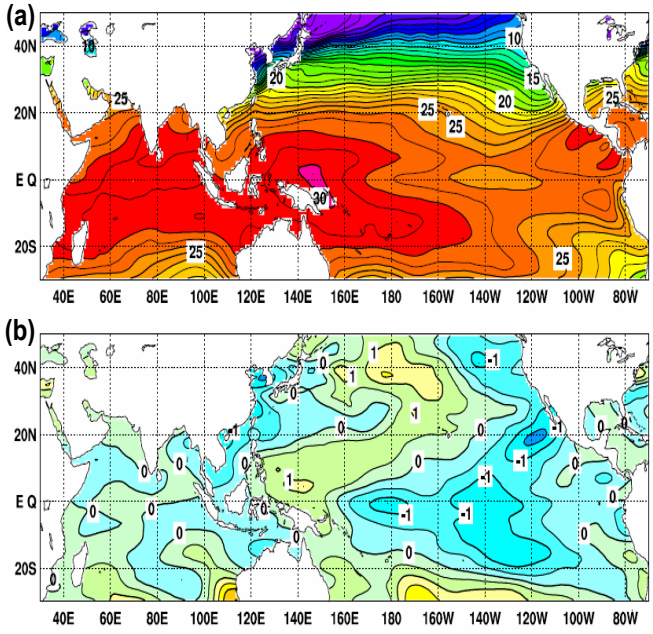

Figure 1 Monthly mean (a) sea surface temperatures (SSTs) and (b) SST anomalies in the Indian and Pacific Ocean areas for March 2011
Contour intervals are 1˚C in (a) and 0.5˚C in (b). The base period for the normal is 1971 – 2000.

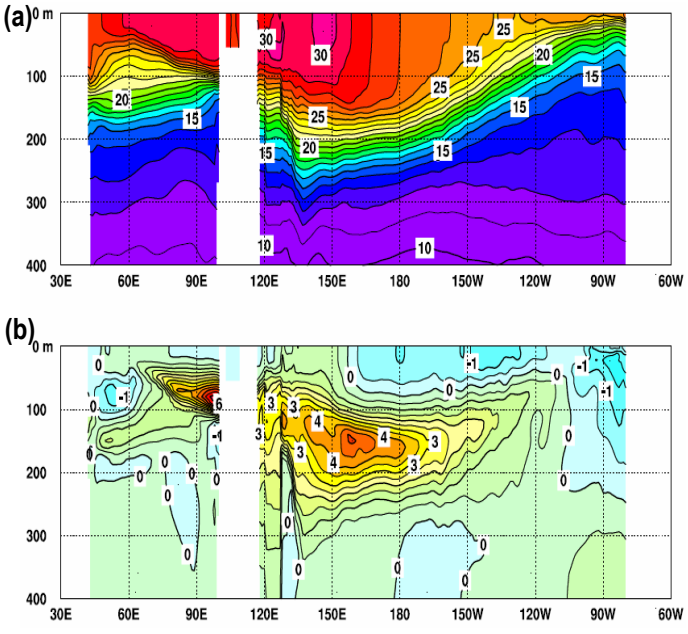

Figure 2 Monthly mean depth-longitude cross sections of (a) temperatures and (b) temperature anomalies in the equatorial Indian and Pacific Ocean areas for March 2011
Contour intervals are 1˚C in (a) and 0.5˚C in (b). The base period for the normal is 1979 – 2004.

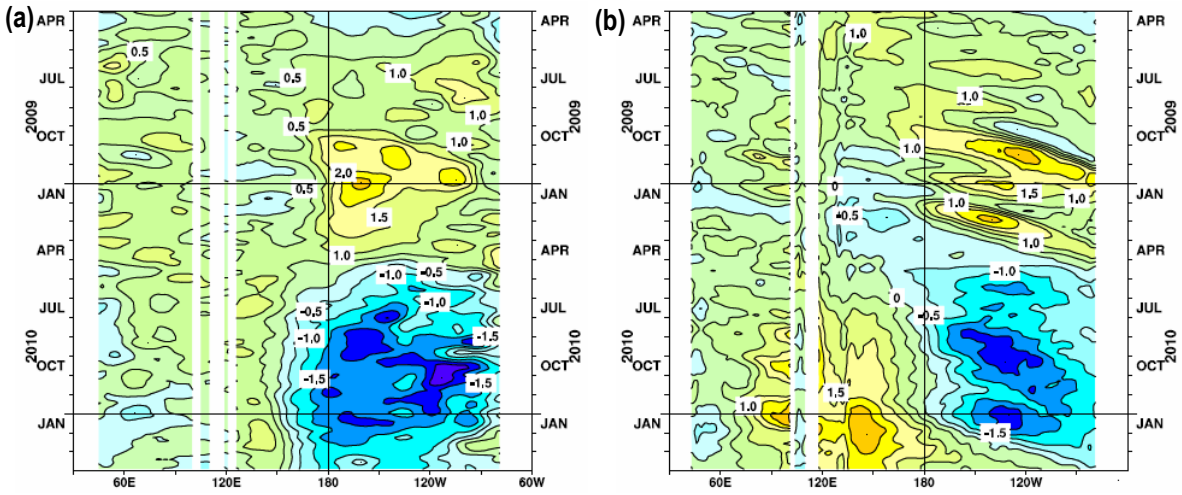

Figure 3 Time-longitude cross sections of (a) SST and (b) ocean heat content (OHC) anomalies along the equator in the Indian and Pacific Ocean areas
OHCs are defined here as vertically averaged temperatures in the top 300 m. The base periods for the normal are 1971 – 2000 for (a) and 1979 – 2004 for (b).

near or above normal during boreal summer, although the uncertainty of the latter half of the prediction period is large (Figure 4).

Considering the above factors, the La Niña conditions that have persisted since last boreal summer are likely to decay in boreal spring, and subsequent neutral conditions are likely to continue in boreal summer, though the level of uncertainty for summer is high.

The SST in the tropical western Pacific (NINO.WEST) region has been above normal since last boreal summer in association with the current La Niña event. It is likely to gradually approach normal levels in the months ahead.

Indian Ocean

The SST averaged over the tropical Indian Ocean (IOBW) region has been below normal since December last year. It is likely to gradually approach normal levels in the months ahead.

(Ichiro Ishikawa, Climate Prediction Division)

* The SST normals for the NINO.WEST region (Eq. – 15° N, 130°E – 150°E) and the IOBW region (20°S – 20°N, 40° E – 100°E) are defined as linear extrapolations with respect to a sliding 30-year period in order to remove the effects of long-term trends.

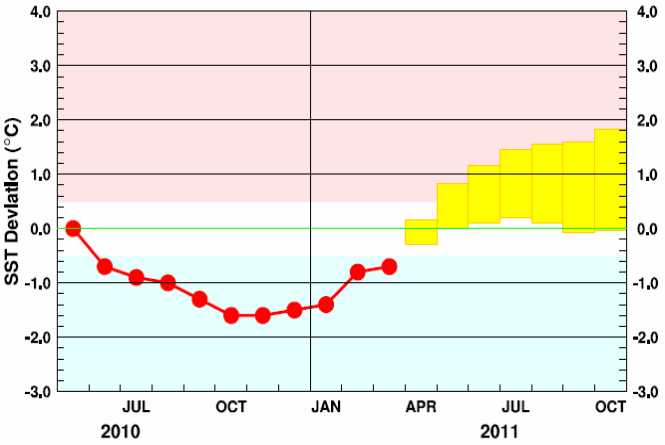

Figure 4 Outlook of the NINO.3 SST deviation produced by the El Niño prediction model
This figure shows a time series of the monthly NINO.3 SST deviations. The thick line with closed circles shows observed SST deviations, and the boxes show the values produced for the next six months by the El Niño prediction model. Each box denotes the range into which the SST deviation is expected to fall with a probability of 70%.

JMA's Seasonal Numerical Ensemble Prediction for Summer 2011

According to JMA's seasonal numerical prediction model, sea surface temperature (SST) anomalies in the eastern equatorial Pacific will be above normal this summer, suggesting a transition from the current La Niña conditions to an El Niño period. Reflecting the predicted El Niño-like SST anomalies, active convection in the central equatorial Pacific and a southward shift of the sub-tropical jet are predicted. However, as prediction skill in relation to El Niño/La Niña conditions from spring through summer is relatively low at the end stage of La Niña periods, it should be noted that the extent of the atmospheric influence from the predicted El Niño-like SST anomalies is uncertain. Conversely, active and inactive convections are predicted to the east of the Philippines and in the tropical Indian Ocean, respectively, reflecting positive anomalies of SSTs in the western tropical Pacific.

1. Introduction

This article outlines JMA's dynamical seasonal ensemble prediction for summer (June – August) 2011, which was used as a basis for the Agency's operational warm-season outlook issued on 25 April 2011. This prediction is based on the seasonal ensemble prediction system used in conjunction with the Atmosphere-Ocean General Circulation Model (AOGCM). Please refer to the separate column for details of the system.

Section 2 outlines the global SST anomaly predictions, and Section 3 describes the circulation fields expected over the tropics and sub-tropics in association with these anomalies. Finally, the circulation fields predicted for the mid- and high latitudes of the Northern Hemisphere are explained in Section 4.

2. SST anomalies (Figure 5)

In March 2011, the NINO.3 region's El Niño monitoring index, which shows the deviation from a sliding 30-year mean SST averaged over this region, was -0.7°C. La Niña conditions have continued since last summer (see also JMA's El Niño Outlook in this issue).

The predicted SST anomalies are shown in Figure 5. Above-normal SSTs are forecast in the eastern equatorial Pacific, suggesting a transition from the current La Niña conditions to an El Niño period. However, hindcast experimentation has indicated that JMA's model tends to predict a quicker transition from La Niña to El Niño conditions than observed values show, and that the prediction skill for El Niño/La Niña conditions from spring through summer is relatively low at the end stage of La Niña periods. Forecasters therefore believe that neutral conditions are likely to be seen this summer. Meanwhile, above-normal SSTs are forecast in the eastern tropical Pacific despite the predicted El Niño-like SST anomalies, though these anomalies are expected to gradually decrease. In the tropical Indian Ocean, normal or slightly above-normal SSTs are predicted.

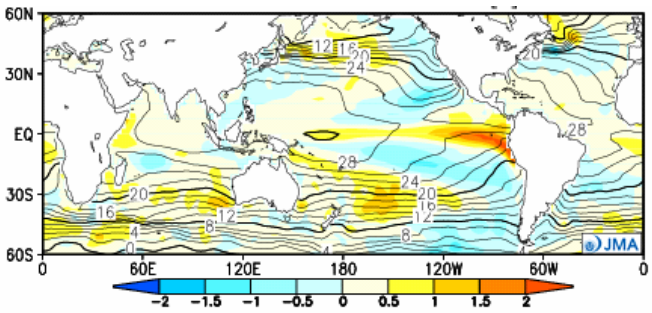

Figure 5 Predicted SSTs (contours) and SST anomalies (shading) for June – August 2011 (ensemble mean of 51 members)

3. Prediction for the tropics and sub-tropics (Figure 6)

Above-normal precipitation is predicted from the central to the eastern equatorial Pacific (a) and to the east of the Philippines (b). Considering the uncertainty of the prediction for a transition to El Niño conditions, the value of the above-normal precipitation in (a) should not be viewed as highly significant. However, the above-normal precipitation in (b) is expected in response to high SSTs over the western tropical Pacific, and the anomaly can be seen as reasonable. Below-normal precipitation is predicted over the Maritime Continent and South Asia.

In the upper troposphere, a negative-velocity potential anomaly at 200 hPa (i.e., more divergent) is predicted over the tropical Pacific, while positive (i.e., more convergent) anomalies are predicted over the tropical Indian Ocean, reflecting the precipitation anomaly patterns in the tropics.

The stream function at 200 hPa is generally expected to be negative in the Northern Hemisphere, reflecting the zonal pattern of precipitation (active near the equator and inactive away from it). This indicates a southward-shifting tendency of the sub-tropical jet. However, considering that these anomalies may reflect predicted El Niño-like SST anomalies, they should not be viewed as highly significant. Positive (i.e., anti-cyclonic) anomalies are predicted to the east of the Philippines, reflecting above-normal precipitation in the region.

Stream function anomalies at 850 hPa are expected to be negative (i.e., cyclonic) to the east of the Philippines and positive (i.e., anti-cyclonic) over South Asia. These anomalies indicate an active western North Pacific monsoon and an inactive Indian monsoon.

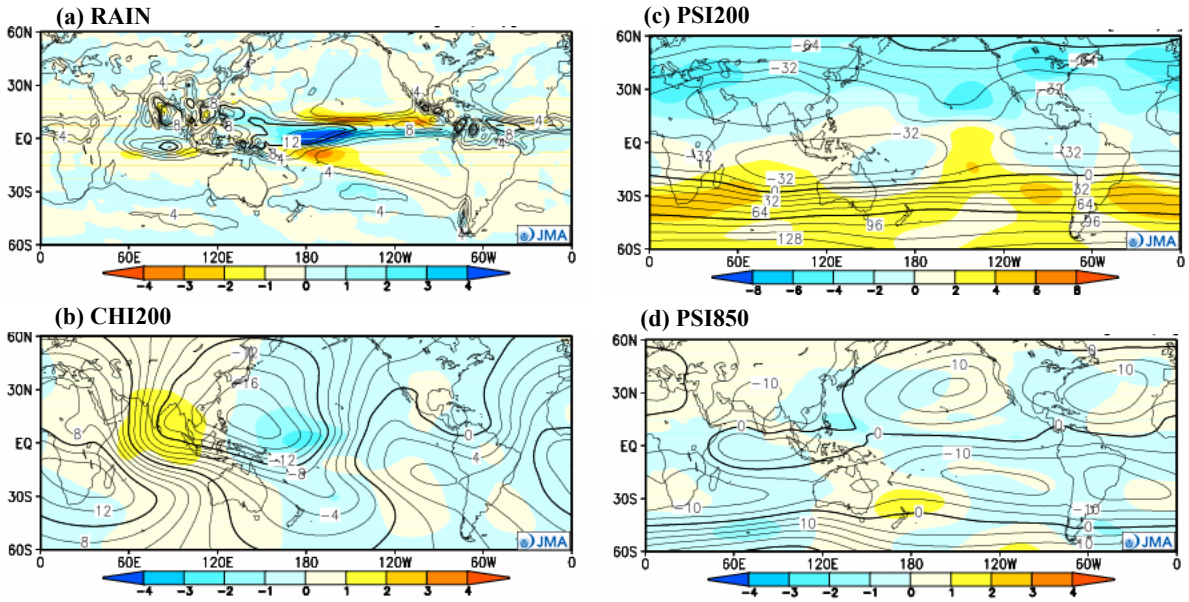

Figure 6 Predicted atmospheric fields from 60°N – 60°S for June – August 2011 (ensemble mean of 51 members)
(a) Precipitation (contours) and anomaly (shading). The contour interval is 2 mm/day.
(b) Velocity potential at 200 hPa (contours) and anomaly (shading). The contour interval is 2×10^6 m^2/s.
(c) Stream function at 200 hPa (contours) and anomaly (shading). The contour interval is 16×10^6 m^2/s.
(d) Stream function at 850 hPa (contours) and anomaly (shading). The contour interval is 5×10^6 m^2/s.

4. Prediction for the mid- and high latitudes of the Northern Hemisphere (Figure 7)

Negative anomalies of sea level pressure are predicted for the western part of the North Pacific High, while positive anomalies are expected in East Asia due to active convection to the east of the Philippines. Geo-potential height anomalies at 500 hPa are expected to be positive over almost the whole of the Northern Hemisphere, implying the influence of the recent warming trend.

(Masayuki Hirai, Climate Prediction Division)

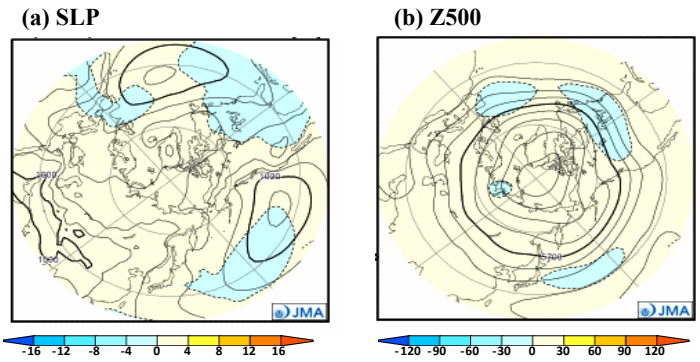

Figures 7 Predicted atmospheric fields from 20°N – 90°N for June – August 2011 (ensemble mean of 51 members)
(a) Sea level pressure (contours) and anomaly (shading). The contour interval is 4 hPa.
(b) 500 hPa height (contours) and anomaly (shading). The contour interval is 60 m.

JMA's Seasonal Ensemble Prediction System

JMA operates a seasonal Ensemble Prediction System (EPS) using the Atmosphere-Ocean General Circulation Model (AOGCM) to make seasonal predictions beyond a one-month time range. The EPS produces perturbed initial conditions by means of a combination of the initial perturbation method and the lagged average forecasting (LAF) method. The prediction is made using 51 members from the latest six initial dates (nine members are run every five days). Details of the prediction system and verification maps based on 30-year hindcast experiments (1979 – 2008) are available at http://ds.data.jma.go.jp/tcc/tcc/products/model/.

Warm Season Outlook for Summer 2011 in Japan

For summer 2011, mean temperatures are likely to be above or near normal in northern Japan and above normal in other regions. Warm-season precipitation amounts are unlikely to exhibit particular features in any region.

1. Outlook summary

In February, JMA issued its outlook for the coming summer over Japan and updated it in March and April. For summer 2011, mean temperatures are likely to be above or near normal in northern Japan with 40% probability for both categories, above normal with 50% probability in other regions. Warm season precipitation amounts are unlikely to exhibit particular features for any region (Figures 8 and 9).

2. Outlook background

JMA's numerical model predicts that SST anomalies averaged over the NINO.3 region will be above normal in summer 2011. However, as the prediction accuracy for NINO.3 SSTs in summer is relatively low at the end stage of La Niña conditions in spring, it is considered that SST anomalies in the region will be mostly near normal in summer. SSTs in the tropical Indian Ocean (IOBW) and in the western equatorial Pacific are both predicted to be slightly above normal in summer 2011.

Three-month precipitation amounts are predicted to be above normal over central and eastern parts of the equatorial Pacific, and atmospheric circulation anomaly patterns over the tropical and sub-tropical Pacific are predicted to be similar to those seen during El Niño conditions. However, the predicted above-normal precipitation amounts are not viewed as highly significant due to the insufficient prediction skill for NINO.3 SSTs.

Positive anomalies of three-month precipitation around and to the east of the Philippines are predicted in association with suppressed convective activity over the tropical Indian Ocean. As a result, the extension of the North Pacific High is predicted to be almost normal around Japan during summer despite the predicted El Niño-like SST anomalies. The Tibetan High is also predicted to be normal. These results indicate that the circulation pattern around Japan will be almost normal in summer.

Conversely, 500-hPa geopotential height anomalies are predicted to be positive over almost the whole of the Northern Hemisphere due to the influence of the recent warming trend. This suggests that summer-averaged temperatures will be above normal in Japan.

(Koji Ishihara, Climate Prediction Division)

Category	−	0	+
Northern Japan	30	30	40
Eastern Japan	20	30	50
Western Japan	20	30	50
Okinawa and Amami	20	30	50

(Category −: below normal, 0 : normal, + : above normal, Unit : %)

Figure 8 Outlook for summer 2011 temperature probability in Japan

Category		−	0	+
Northern Japan	Sea of Japan side	30	30	40
	Pacific side	30	30	40
Eastern Japan	Sea of Japan side	30	40	30
	Pacific side	30	40	30
Western Japan	Sea of Japan side	30	40	30
	Pacific side	30	40	30
Okinawa and Amami		30	40	30

(Category −: below normal, 0 : normal, + : above normal, Unit : %)

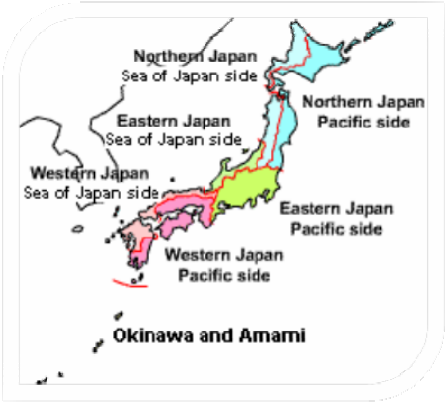

Figure 9 Outlook for summer 2011 precipitation probability in Japan

Summary of Asian Winter Monsoon 2010/2011

Surface climate conditions

In winter 2010/2011, intra-seasonal variations of temperature anomalies were clear except in southern Asia (Figure 10). Lower-than-normal temperatures were observed around central Siberia in December, while higher-than-normal temperatures were seen around its northern and southern parts in January and February, respectively. Also, lower-than-normal temperatures were observed around China in January, while this area experienced higher-than-normal temperatures in February. These temperature differences were affected by pronounced intra-seasonal variations of the Siberian High (see *Conditions of atmospheric circulation*).

Figure 11 shows extreme climate events that occurred from December 2010 to February 2011. In December, extremely low temperatures were observed around central Siberia, while extremely high temperatures were seen around the South China Sea. Moreover, extremely heavy precipitation (snow) was observed from eastern Mongolia to Japan. In January, extremely low temperatures were observed around China, and extremely light precipitation was seen from the southern part of western Siberia to the eastern part of central Asia and from the Pacific side of Japan to the southern part of the Korean Peninsula. In February, heavy precipitation (snow) was observed from southern Kazakhstan to Pakistan.

(Takafumi Umeda, Climate Prediction Division)

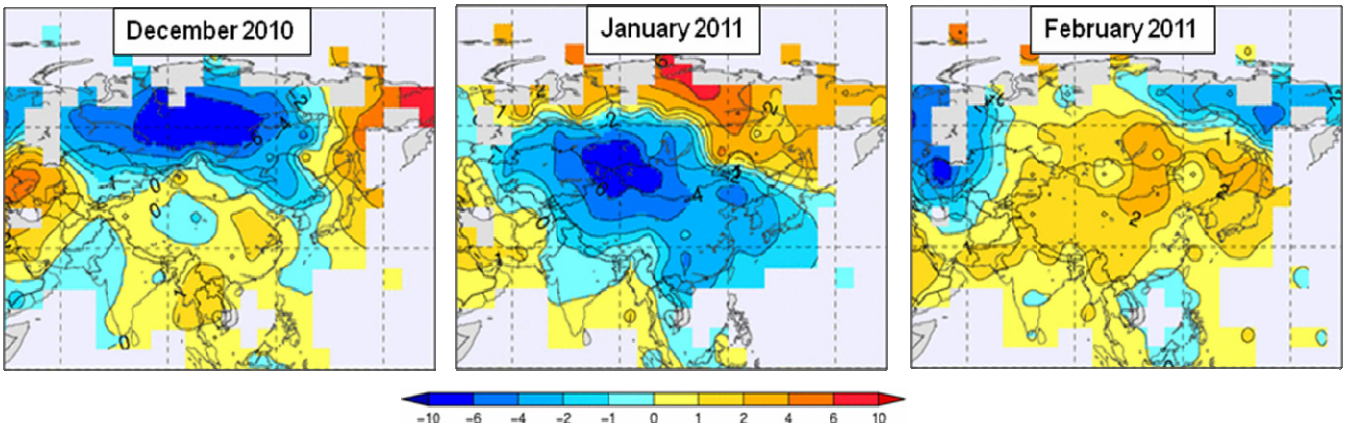

Figure 10 Monthly temperature anomalies from December 2010 to February 2011
Anomalies are deviations from the normal (i.e., the 1971 – 2000 average). The contour interval is 1°C.

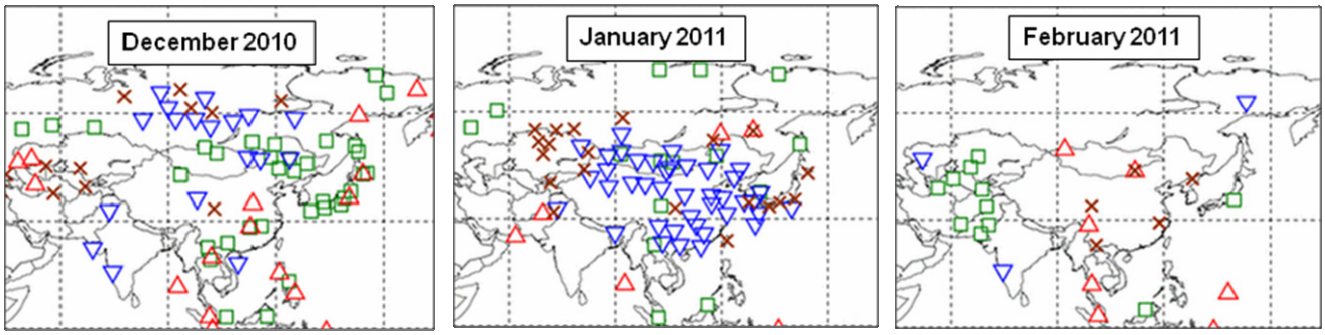

Figure 11 Extreme climate events from December 2010 to February 2011

△ Extremely high temperature (ΔT/SD≧ 1.83)
▽ Extremely low temperature (ΔT/SD≦ −1.83)
□ Extremely heavy precipitation (Rd=6)
× Extremely light precipitation (Rd=0)

Conditions of atmospheric circulation

In the 500-hPa height field for boreal winter 2010/2011 (December 2010 – February 2011), positive and negative height anomalies were generally seen in the high and middle latitudes of the Northern Hemisphere, respectively, indicating a negative Arctic Oscillation (AO) phase (Figure 12). The AO remained in a significantly negative phase during the first half of winter 2010/2011, turning positive in the second half (Figure 13). The Siberian High was stronger than normal around its center, and the Aleutian Low was obscure (Figure 12). The Siberian High was significantly strengthened in January and March 2011, while it was weakened in December 2010 and February 2011, showing that its intra-seasonal variation was pronounced in the winter monsoon season (Figure 14). In the tropics, the La Niña event that started in summer 2010 continued into the winter. In association with this, convective activity was enhanced from the eastern Indian Ocean to the Maritime Continent, while it was suppressed across the western and central equatorial Pacific (Figure 15).

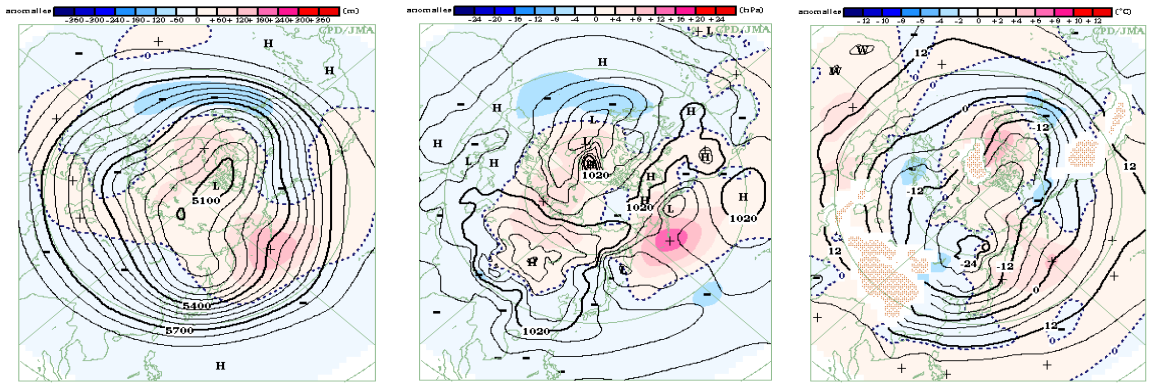

Figure 12 Three-month averaged 500-hPa height (left), sea level pressure (center) and 850-hPa temperature (right) for December 2010 – February 2011

The shading indicates anomalies, and the wavy hatch patterns indicate areas with altitudes higher than 1,600 m. The base period for the normal is 1979 – 2004. JRA/JCDAS data were used in the analysis.

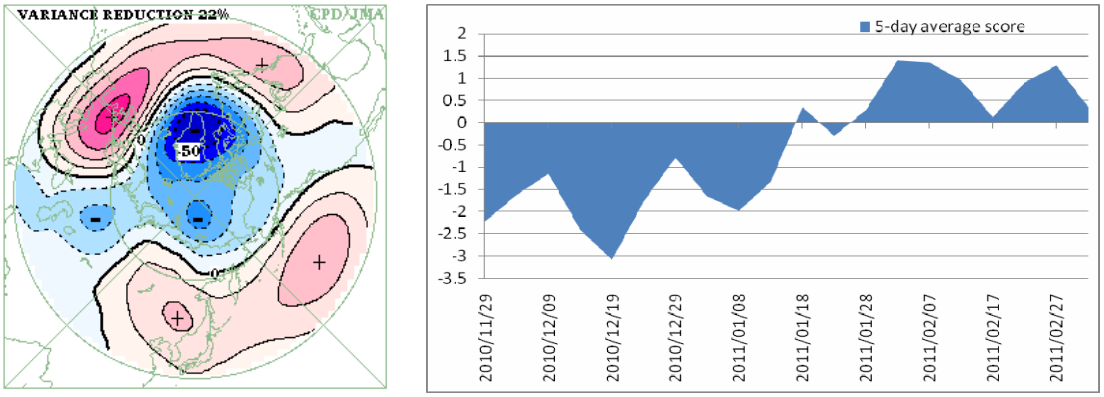

Figure 13 First mode of empirical orthogonal function (EOF) analysis for three-month mean 500-hPa height in the Northern Hemisphere (30˚N – 90˚N) for December – February (left), and time series of EOF scores in boreal winter 2010/2011 (right)

Left: the contours show the distribution of values obtained by multiplying the eigenvector of the first mode by the root of the corresponding eigenvalue (unit: m). EOF analysis was conducted using a covariance matrix for 47 samples from between 1958 and 2004. ERA-40 data (1958 – 1978) and JRA/JCDAS data (1979 – 2004) were used in the analysis; right: the values show the normalized EOF scores obtained by dividing EOF scores (calculated by projecting the five-day mean 500-hPa height anomalies onto the eigenvector) by the root of the corresponding eigenvalue.

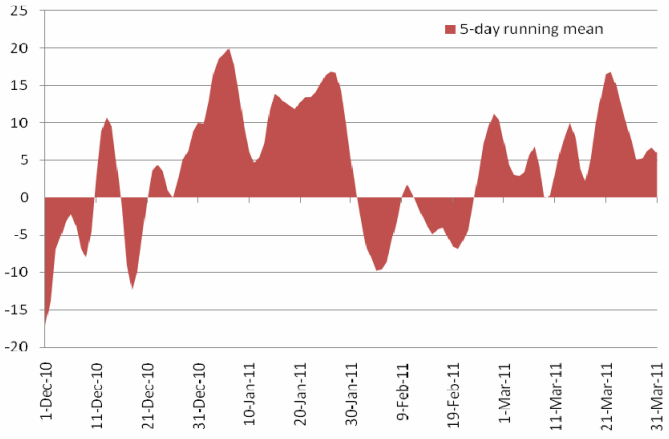

Figure 14 Time series of intensity for the Siberian High from December 2010 to March 2011

The values indicate five-day running means of area-averaged sea level pressure anomalies (unit: hPa) to the southwest of Lake Baikal (45˚N – 55˚N, 90˚E – 105˚E). The base period for the normal is 1979 – 2004. JRA/JCDAS data were used in the analysis.

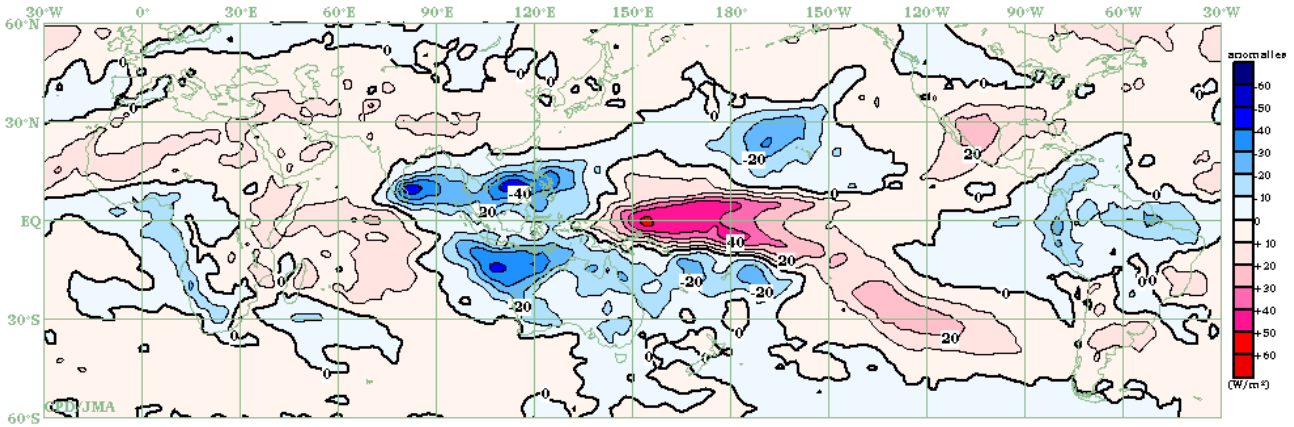

Figure 15 Three-month averaged outgoing longwave radiation anomaly for December 2010 – February 2011
The warm/cold-color shading indicates weaker/stronger-than-normal convective activity. The base period for the normal is 1979 – 2004. Original OLR data were provided by NOAA.

Strong East Asian winter monsoon in January 2011

During late December 2010 and January 2011, the East Asian winter monsoon was significantly enhanced, leading to extremely low temperatures over wide areas of East Asia (Figure 16). Japan experienced below-normal January temperatures nationwide for the first time since 1986, as well as heavy snowfall on the Sea of Japan side of the country. In the upper troposphere, ridges were seen over the western part of Siberia, and blocking highs developed over the eastern part in January (Figure 16). These conditions were suitable for the enhancement of the Siberian High. The Aleutian Low was enhanced to the east of Japan in January (Figure 16), although it was obscure in December and February. The pronounced Siberian High and Aleutian Low led to a strong winter monsoon over East Asia in January.

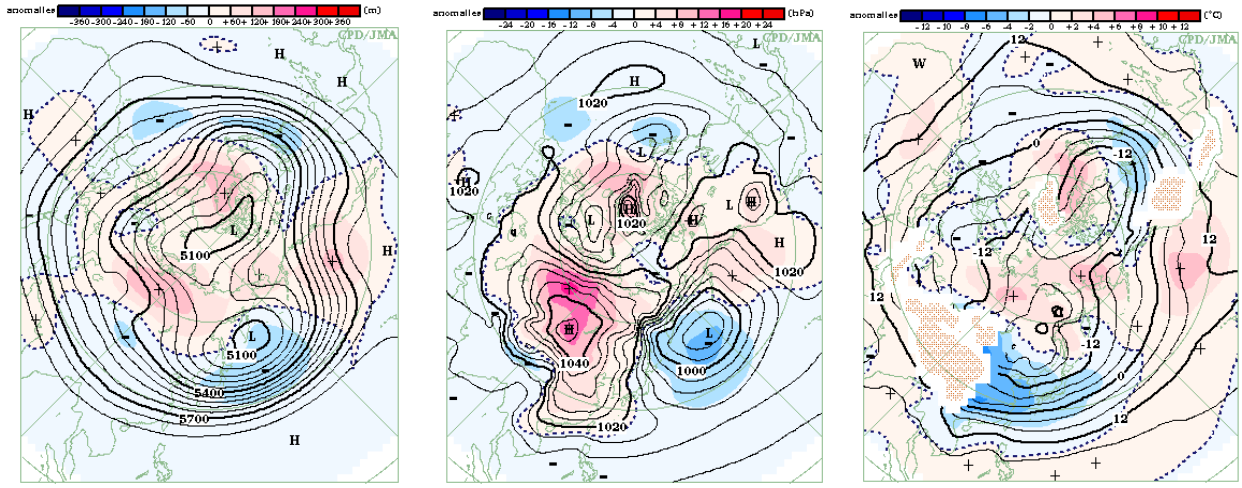

Figure 16 Monthly averaged 500-hPa height (left), sea level pressure (center) and 850-hPa temperature (right) for January 2011
The shading indicates anomalies, and the wavy hatch patterns indicate areas with altitudes higher than 1,600 m. The base period for the normal is 1979 – 2004. JRA/JCDAS data were used in the analysis.

Significant cold surges around the South China Sea in March 2011

The Siberian High was significantly developed in March (Figure 14). Focusing on the details, high surface pressure to the southwest of Lake Baikal peaked around 20 March with an extremely cold air mass in the lower troposphere (Figure 17). Thereafter, high-pressure anomalies related to this cold air mass propagated southward along the eastern periphery of the Tibetan Plateau and reached the South China Sea and the Indochina Peninsula late in the month, bringing significant cold surges. In conjunction with these surges, convective activity was enhanced over the South China Sea and the Indochina Peninsula as well as over the Maritime Continent, where it was strengthened due to the La Niña event. The intensity of northerly surges around the South China Sea was the strongest for March since 1979 (Figure 18).

(Shotaro Tanaka, Climate Prediction Division)

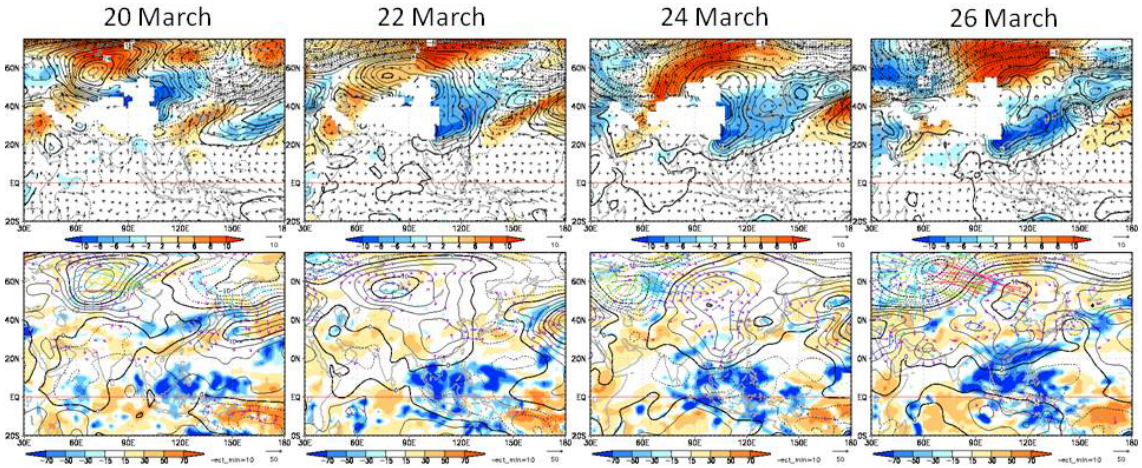

Figure 17 Evolution of cold surges around the South China Sea
The upper panels show anomalies of 10-m wind vectors (unit: m/s), sea level pressure at intervals of 4 hPa (contours) and 850-hPa temperature at intervals of 2˚C (shading); the lower panels indicate 850-hPa wave activity fluxes (unit: m^2/s^2), anomalies of 850-hPa stream function at intervals of 2.5 × 10^6 m^2/s and outgoing longwave radiation (unit: W/m^2).

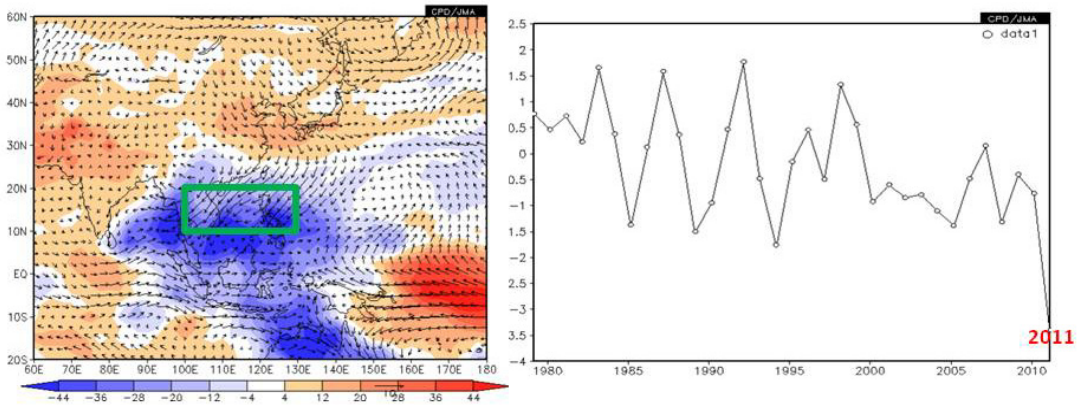

Figure 18 Time series of intensity for cold surges around the South China Sea for March from 1979 to 2011
Left: monthly mean outgoing longwave radiation anomalies at intervals of 8 W/m^2 (shading) and 925-hPa wind vector anomalies (unit: m/s) for March 2011; right: time series of 925-hPa meridional wind speed anomalies averaged around the South China Sea (10˚N – 20˚N, 100˚E – 130˚E: the area shown by the green rectangle in the panel on the left), and negative (positive) values indicate northerly (southerly) wind anomalies.

Stratospheric Circulation in Winter 2010/2011

In winter 2010/2011, the polar vortex was stronger than normal, and lower-than-normal temperatures were generally seen at the 30-hPa level over the North Pole. Two minor stratospheric sudden warming (SSW) events occurred, but did not reach the criteria for categorization as major events. This section reports on the characteristics of stratospheric circulation seen during this winter.

Characteristics of stratospheric circulation

Temperatures at 30 hPa over the North Pole remained below normal during almost the whole period from mid-November 2010 to March 2011, and were remarkably below normal from mid-February to mid-March in particular. The minimum value was observed in mid-February, while in the climatological normal it is seen in the period from late December to early January (Figure 19). In the three-month mean 30-hPa height field from December 2010 to February 2011 (Figure 20 (a)), the polar vortex was stronger than normal with negative anomalies over the Arctic region, which was the opposite of the patterns seen in winter 2009/2010 (Figure 20 (b)) and 2008/2009 (Figure 20 (c)) when a major SSW event occurred (Harada et al. 2010).

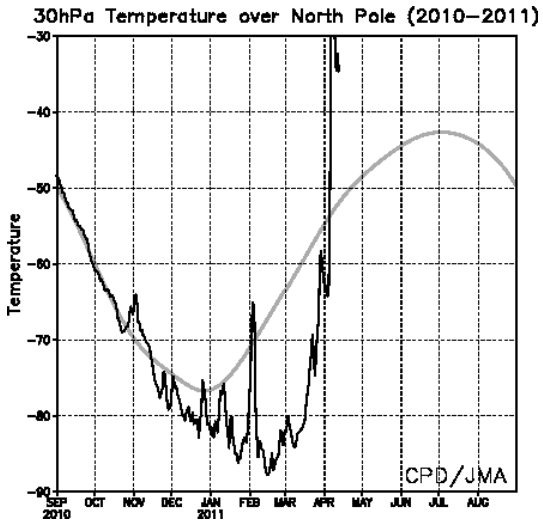

Figure 19 Time series of temperatures at the 30-hPa level over the North Pole (September 2010 – April 2011)
The black line shows daily temperatures, and the gray line indicates the climatological mean.

In winter 2010/2011, two minor SSW events occurred in the first half of January and in the period from late January to early February. In the first event, an anticyclone developed around Alaska, and the polar vortex shifted moderately toward Europe and the Atlantic, showing a pronounced planetary wave of zonal wavenumber 1 (Figure 21 (a)). However, the anticyclone did not extend broadly over the Arctic region. In the second event, the planetary wave of zonal wavenumber 2 was pronounced following that of zonal wavenumber 1 (Figure 21 (b)). The two centers of the polar vortex were seen over the Atlantic and Russia, but it did not form two clearly split vortices. The vertical component of the Eliassen-Palm flux (EP flux; after Palmer, 1982) averaged over 30° – 90°N at the 100-hPa level was remarkable in the first half of the last 10-day period of January with planetary waves of zonal wavenumber 1 and in the second half of the same period with planetary waves of zonal wavenumber 2 (Figure 22 (c)). Considering that the vertical component of the EP flux indicates the vertical propagation of energy by planetary waves, it can be inferred that the planetary wave of zonal wavenumber 2 propagated from the troposphere to the stratosphere following the propagation of the planetary wave of zonal wavenumber 1. When the two SSW events occurred, zonal-mean 30-hPa westerly winds at 60°N weakened, but did not turn easterly (Figure 22 (b)).

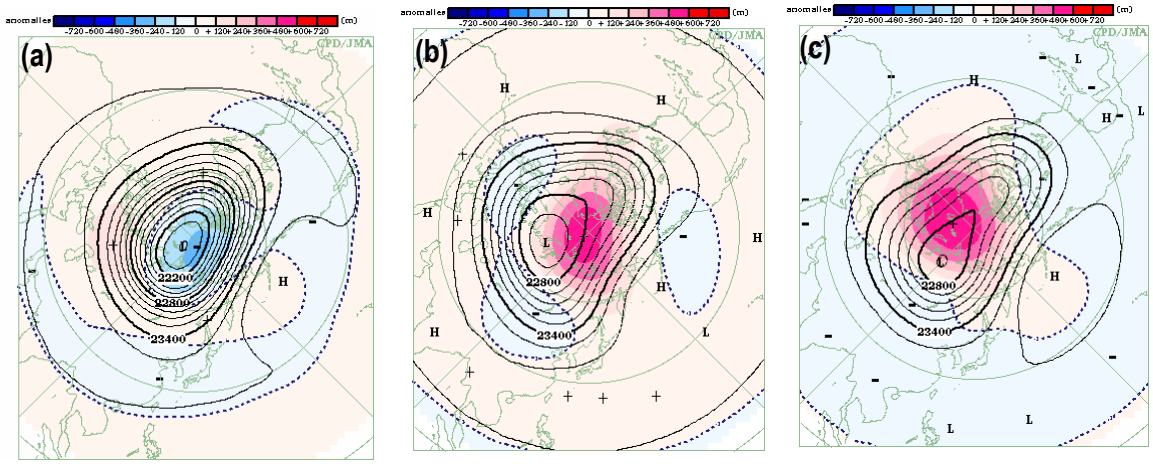

Figure 20 Three-month mean 30-hPa height and anomaly in the Northern Hemisphere for (a) December 2010 – February 2011, (b) December 2009 – February 2010, and (c) December 2008 – February 2009
The contours show 30-hPa height at intervals of 120 m, and the shading indicates its anomaly.

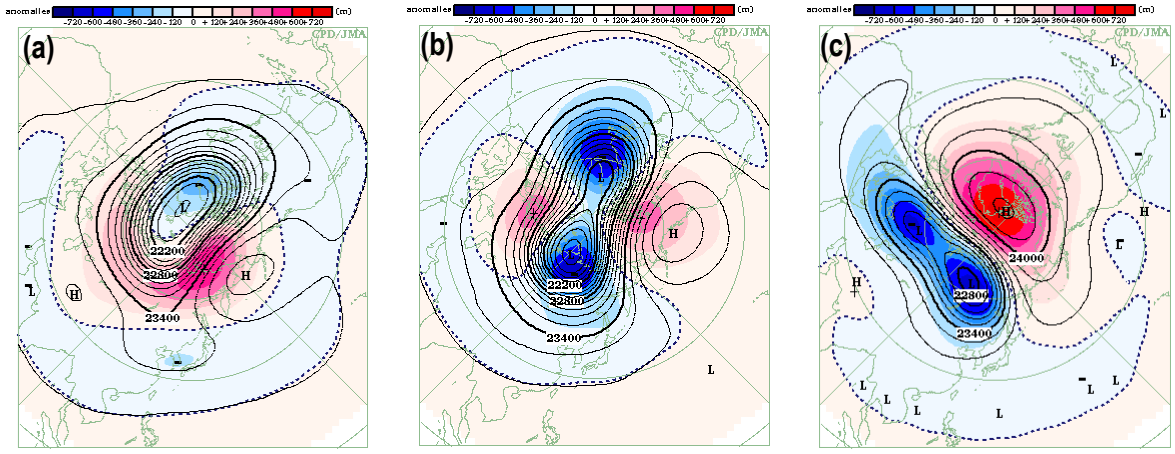

Figure 21 Five-day mean 30-hPa height and anomaly in the Northern Hemisphere for (a) 11 – 15 January, (b) 31 January – 4 February, and (c) 11 – 15 April 2011
The contours show 30-hPa height at intervals of 120 m, and the shading indicates its anomaly.

Final warming

The increase of the 30-hPa temperature over the North Pole was significant in late March, and the temperature rapidly rose in early April (Figures 19 and 22 (a)). In this period, an anticyclone formed around Alaska, and gradually developed and extended over the polar region (Figure 21 (c)). In mid-April, zonal-mean 30-hPa winds at 60°N turned from westerlies to easterlies (Figure 22 (b)), and an anticyclonic circulation (a normal formation in the stratosphere during the summer season) appeared over the polar region.

(Nobuyuki Kayaba, Climate Prediction Division)

Reference

Harada, Y., A. Goto, H. Hasegawa, N. Fujikawa, H. Naoe and T. Hirooka, 2010: A major stratospheric sudden warming event in January 2009. *J. Atmos. Sci.*, **67**, 2052-2069. doi: 10.1175/2009JAS3320.1.

Palmer, T. N., 1982: Properties of the Eliassen-Palm flux for planetary scale motions. *J. Atmos. Sci.*, **39**, 992-997.

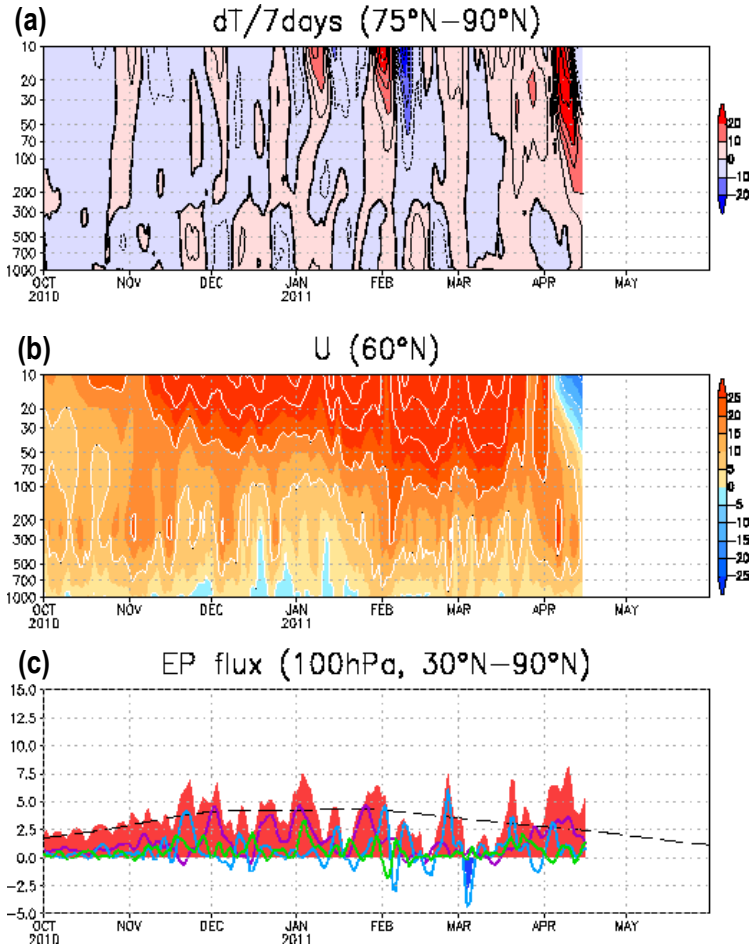

Figure 22 (a) Time-height cross section for seven-day variations of zonal mean temperature averaged over 75° – 90°N, (b) time-height cross section of zonal mean zonal wind at 60°N, and (c) time series of vertical components of EP flux averaged over 30° – 90°N at the 100-hPa level (October 2010 – April 2011)
The red bars in (c) denote the vertical component of EP flux for whole zonal wave numbers. The purple, light-blue and light-green lines denote the vertical components of EP flux for zonal wavenumbers 1, 2 and 3, respectively. The broken line in (c) denotes the climatological mean for the vertical component of EP flux for whole zonal wavenumbers. The unit for the vertical component of EP flux in (c) is m^2/s^2.

JMA's New Climatological Normals for 1981 – 2010

1. Introduction

Climatological normals are used as a base for comparison of current conditions, as well as to describe average climatic conditions. Under the Technical Regulations of the World Meteorological Organization (WMO-No. 49), climatological standard normals are averages of climatological data computed for the following consecutive 30-year periods: 1 January, 1901, to 31 December, 1930; 1 January, 1931, to 31 December, 1960, etc. Countries should calculate climatological standard normals as soon as possible after the end of a standard normal period. Although not required by WMO, many countries including Japan update their climatological normals every decade.

JMA has developed new climatological normals using climatological data for the period from 1981 to 2010, and started operationally using them on 18 May, 2011. The climatological normals specified below are used in a number of products available on the TCC website. Some of their details are summarized in the following sections.

- Monthly climatological normals of surface observation stations in Japan as used in products available in the Climate in Japan section (Section 2)

- Monthly climatological normals of surface observation stations around the world (temperature and precipitation) as used in products available in the World Climate section (Section 3)

- For global mean surface temperature, anomalies for individual surface observations are calculated in relation to the 1971 – 2000 average before being averaged over the globe and adjusted to the 1981 – 2010 reference period (Section 4).

- Climatological normals of oceanographic data based on Daily Sea Surface Analysis for Climate Monitoring and Predictions (COBE-SST) and the Ocean Data Assimilation System (MOVE/MRI.COM-G) as used in products available in the El Niño Monitoring section (Section 5)

- Climatological normals of atmospheric circulation fields calculated using data of the Japanese 25-year Reanalysis (JRA-25) and the JMA Climate Data Assimilation System (JCDAS) as used in products available in the Climate System Monitoring section (Details of this section will be given in the next issue of TCC News.)

(Teruko Manabe and Ryuji Yamada, Tokyo Climate Center)

2. Climatological normals of surface observation stations in Japan

Table 1 shows the differences between new and old climate normals for seasonal and annual mean temperatures in each region. It can be seen that the new values tend to be 0.2 − 0.3ºC higher than the old ones for most seasons and regions.

Table 2 shows the ratios of new to old normals for seasonal and annual precipitation amounts in each region. There seems to be no common trend of change for any season or region. However, the increase in winter on the Pacific side of eastern Japan and the decrease in autumn on the Pacific side of western Japan are especially significant.

(Koji Ishihara, Climate Prediction Division)

Table 1 Differences between new and old climate normals for seasonal and annual mean temperatures (unit: ºC)
Positive values indicate new normals higher than old ones.

	Winter (Dec.− Feb.)	Spring (Mar. − May)	Summer (Jun.− Aug.)	Autumn (Sep. – Nov.)	Annual (Jan. – Dec.)
Northern Japan	+0.2	+0.3	+0.1	+0.3	+0.2
Eastern Japan	+0.3	+0.3	+0.3	+0.3	+0.3
Western Japan	+0.2	+0.3	+0.3	+0.4	+0.3
Okinawa and Amami	+0.3	+0.1	+0.2	+0.3	+0.2

Table 2 Ratios of new to old normals for seasonal and annual precipitation amounts (unit: %)

	Winter (Dec.− Feb.)	Spring (Mar. − May)	Summer (Jun.− Aug.)	Autumn (Sep. – Nov.)	Annual (Jan. – Dec.)
Sea of Japan side of northern Japan	101	99	101	99	100
Pacific side of northern Japan	101	98	103	97	100
Sea of Japan side of eastern Japan	100	100	99	98	99
Pacific side of eastern Japan	106	100	100	102	101
Sea of Japan side of western Japan	100	101	98	99	99
Pacific side of western Japan	102	100	98	96	99
Okinawa and Amami	97	96	98	103	99

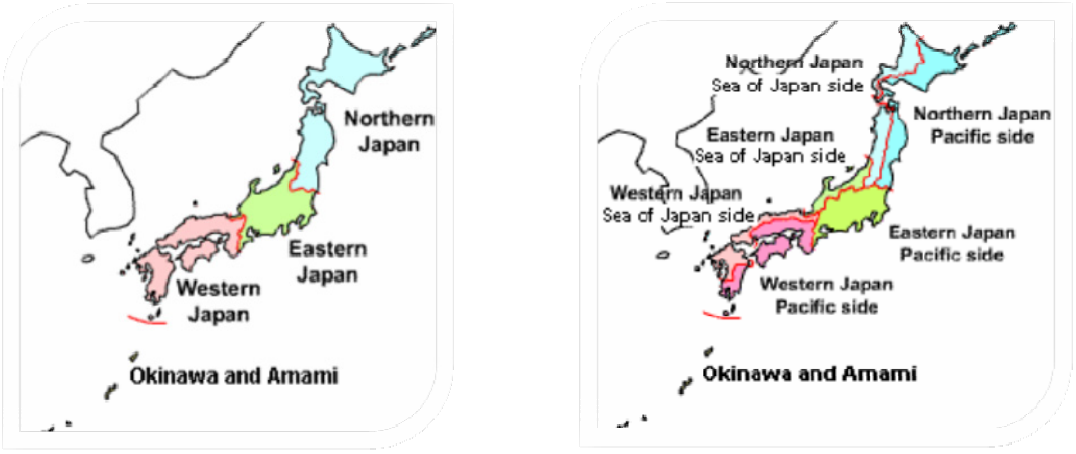

Figure 23 Regionalization for temperatures (left) and precipitation amounts (right)

3. World climatological normals

JMA has started using new climatological normals covering the period from 1981 to 2010 to monitor the world climate.

As before, both data from CLIMAT bulletins and those from the GHCN-Monthly database produced by NOAA/NCDC were used to produce the new normals. Now, JMA's CLIMAT dataset (covering the period from June 1982 to present) includes almost the whole statistical period of the normals (1981 – 2010). Accordingly, if both CLIMAT and GHCN-Monthly data are available for a station, CLIMAT data take priority.

Comparison between the new and old normals

There are 2,549 surface temperature stations and 2,658 precipitation stations (except for Japanese stations) for which new climatological normals could be calculated (Figure 24). The new number of normal-temperature stations is larger than the old one (2,025), while the new number of normal-precipitation stations is smaller (3,800).

The new normal temperatures are higher than the old ones at most stations for every month. However, no distinctive differences extend over wide areas or for several consecutive months between the new and old normal precipitation amounts. Figure 25 shows the differences between the new and old normal temperatures and the ratio of new to old precipitation normals for January and July.

(Takafumi Umeda, Climate Prediction Division)

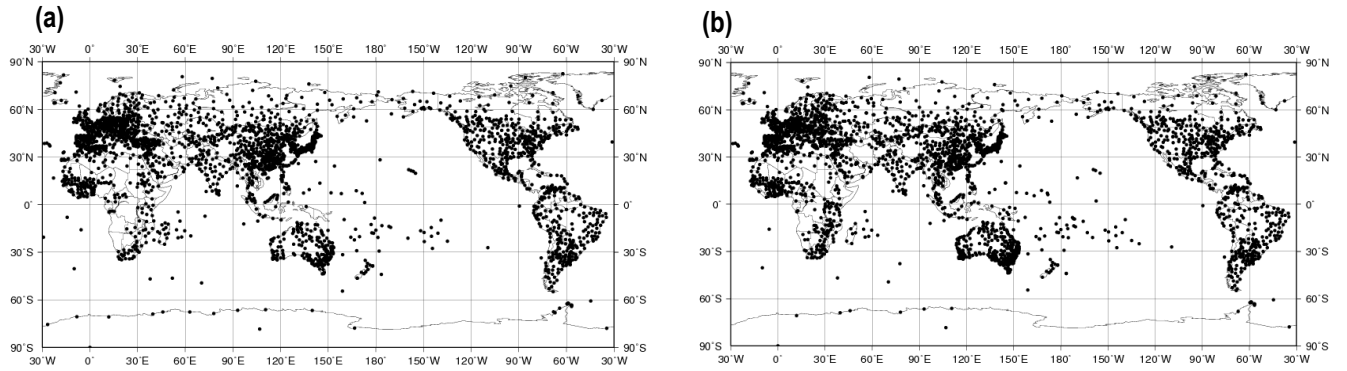

Figure 24 Distributions of climatological-normal stations for (a) surface temperature and (b) precipitation
Only stations with at least eight observations for every month from 1981 to 2010 are plotted on each map.

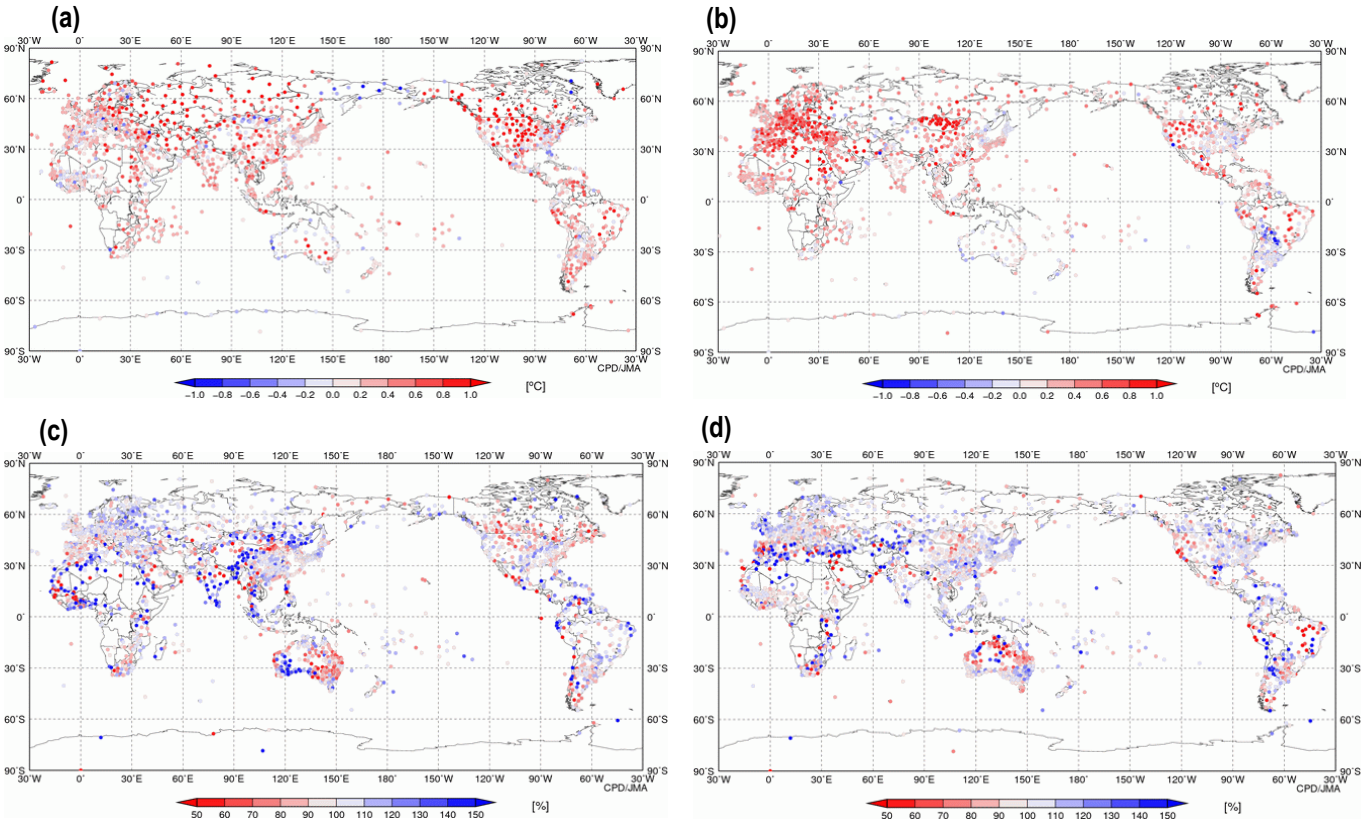

Figure 25 Differences between JMA's new and old normal temperatures for (a) January and (b) July, and ratios of new to old precipitation normals for (c) January and (d) July

4. Global Mean Surface Temperature

With a changing climate system in which most of the warming observed since the mid-20th century is very likely attributable to increased anthropogenic greenhouse concentration (IPCC, 2007), it is increasingly important for policy makers and the general public to be kept informed of the state of the Earth. As one of the world's leading climate centers, JMA reports on the global mean surface temperature (i.e., the combined average of near-surface air temperatures over land and sea surface temperatures) on a monthly, seasonal and annual basis, thereby helping to raise public awareness of climate change.

For the new decade starting from 2011, JMA has replaced the reference period against which global mean temperature anomalies are operationally calculated. As of May 2011, the global temperature is presented as the departure from the 1981 – 2010 average as opposed to the previous period of 1971 – 2000. Anomalies for individual stations are still calculated in relation to the 1971 – 2000 average, as this period has wider coverage for historical observations. For the global mean temperature, however, the baseline period has been adjusted to 1981 – 2010, which is expected to better reflect how the climate is experienced by those living in today's age of global warming. However, one point should be noted; the global mean temperature anomaly for the year 2010, for example, was reported to be +0.34°C in relation to the 1971 – 2000 average (see TCC News No. 23), whereas anomalies for 2011 and several years thereafter are highly likely to fall within a range significantly below this figure. This is not because the Earth has mysteriously stopped warming and started cooling; it is simply because temperatures will be shown in relation to the warmer era of 1981 – 2010.

In addition to the reference period change, time-series graph products from JMA have undergone a number of appearance improvements. In place of the light-blue and pink candlesticks that previously represented temperature anomalies for individual years (Figure 26), simple line plots are adopted in the new design (Figure 27). This revised form is expected to help highlight trends on a decades-to-century time scale rather than year-to-year and month-to-month fluctuations. In the context of monitoring global climate change, which is gradually developing against a backdrop of greater variability, the longer-term tendency is more relevant than the fluctuations inherent in the natural climate system.

(Yoshinori Oikawa, Climate Prediction Division)

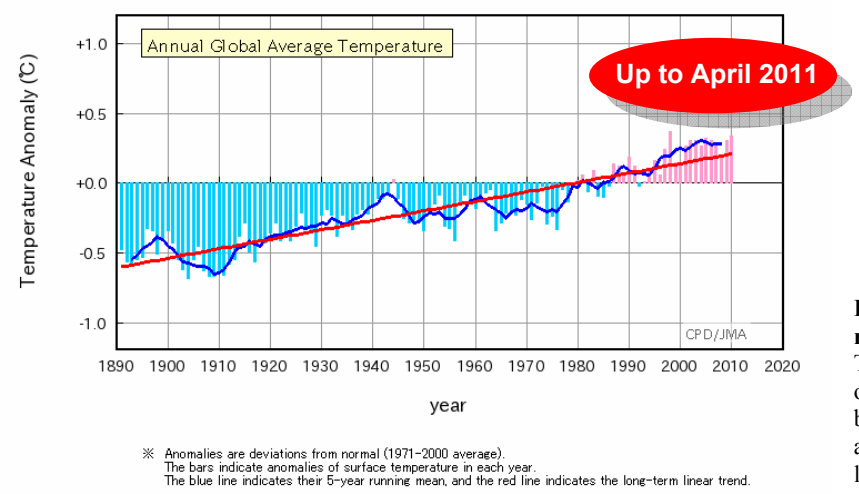

Figure 26 Surface temperature anomalies relative to the 1971 – 2000 average
The light-blue and pink bars indicate anomalies of surface temperature for individual years. The blue line indicates the five-year running mean, and the straight red line shows the long-term linear trend.

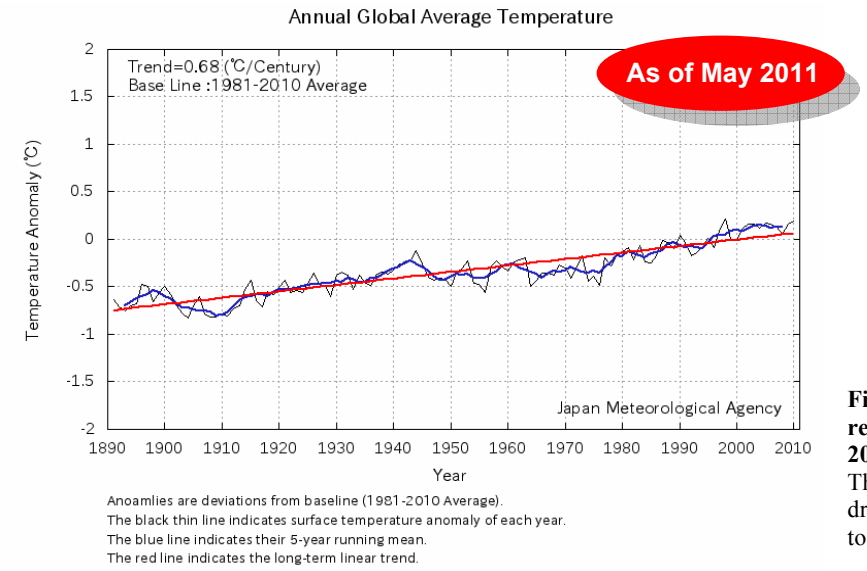

Figure 27 Surface temperature anomalies relative to the new baseline period of 1981 – 2010
The new form of graph product is expected to draw more attention to the long-term trend than to year-on-year variability.

5. Climatological normals of oceanographic data

(1) Sea surface temperatures

Climatologies of monthly sea surface temperatures (SSTs) have been updated using the average for the period from 1981 to 2010 instead of 1971 to 2000. From now on, SST anomalies will be expressed as departures from this new period.

Figure 28 shows differences between the new and old monthly SST climatologies for January and July. The new ones show higher values in the tropical Indian Ocean, the tropical Pacific and the North Atlantic, and higher values in the Arctic Ocean in summer.

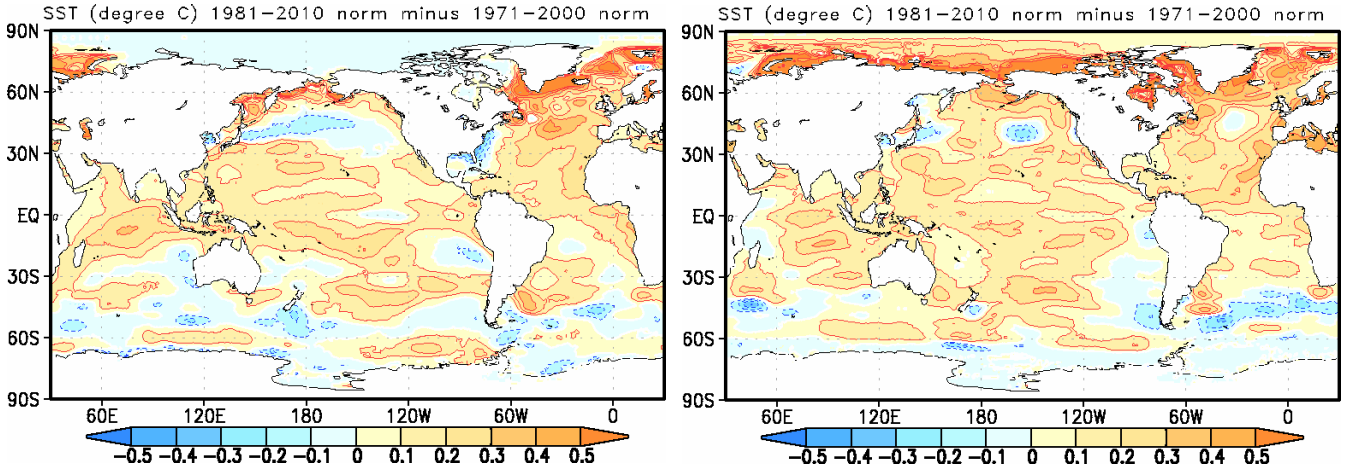

Figure 28 Differences between new and old monthly SST climatologies for January (left) and July (right)

(2) Subsurface water temperatures

JMA operationally analyzes ocean subsurface temperatures based on the ocean data assimilation system (MOVE/MRI.COM-G) for the purpose of monitoring El Niño events. The subsurface temperature normal has also been updated using the data from 1981 to 2010 instead of those from the period 1979 – 2004.

Ocean heat content (OHC) in the new normals is lower in the eastern tropical Pacific and the west of North and South America and higher in other areas (Figure 29 (a)). The global mean difference in OHC from the old normal is about 0.03°C. In the equatorial Pacific, subsurface water temperatures in the new normal are higher in the western equatorial Pacific and lower in the eastern equatorial Pacific than with the old normal (Figure 29 (b)).

(Akio Narui and Hiroyuki Sugimoto, Climate Prediction Division)

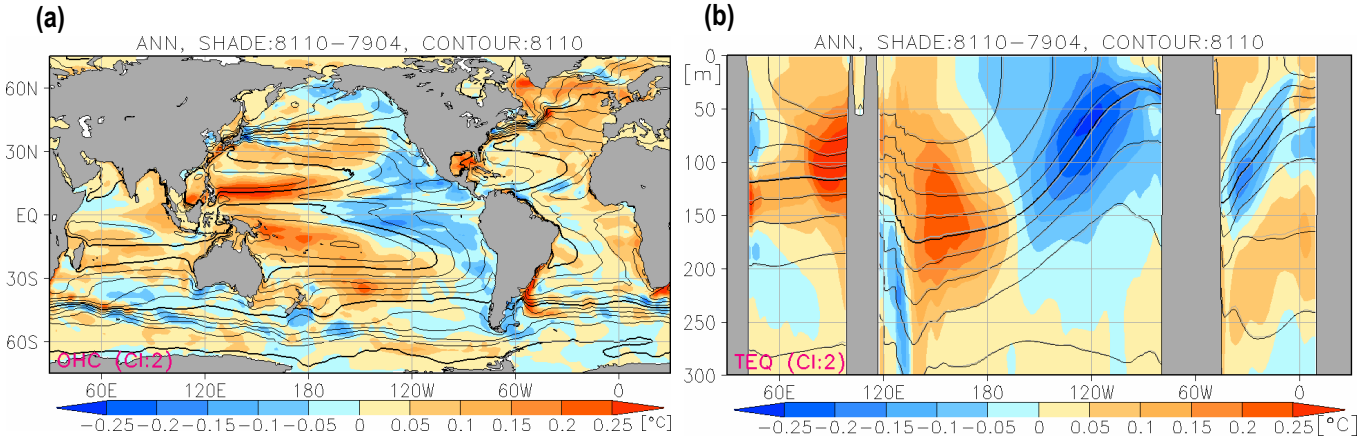

Figure 29 (a) Annual mean ocean heat content and (b) depth-longitude cross sections of temperatures along the equator
The black contours show values for the 1981 – 2010 normal. The grey contours in (b) are for the 1979 – 2004 normal. The contour interval is 2°C, and shading shows differences between the new and old normals.

Any comments or inquiries on this newsletter and/or the TCC website would be much appreciated. Please e-mail to: tcc@met.kishou.go.jp
(Editors: Teruko Manabe, Ryuji Yamada, Kenji Yoshida)

Tokyo Climate Center (TCC), Climate Prediction Division, JMA
Address: 1-3-4 Otemachi, Chiyoda-ku, Tokyo 100-8122, Japan
TCC website: http://ds.data.jma.go.jp/tcc/tcc/index.html